

Gedunin abrogates aldose reductase, PI3K/Akt/mToR, and NF- κ B signaling pathways to inhibit angiogenesis in a hamster model of oral carcinogenesis

Kranthi Kiran Kishore T¹ · Raghu Ganugula² · Deepak Reddy Gade³ · Geerreddy Bhanuprakash Reddy² · Siddavaram Nagini¹

Received: 10 July 2015 / Accepted: 25 August 2015 / Published online: 5 September 2015
© International Society of Oncology and BioMarkers (ISOBM) 2015

Abstract Aberrant activation of oncogenic signaling pathways plays a central role in tumor development and progression. The aim of this present study was to investigate the chemopreventive effects of the neem limonoid gedunin in the hamster model of oral cancer based on its ability to modulate aldose reductase (AR), phosphatidyl inositol-3-kinase (PI3K)/Akt, and nuclear factor kappa B (NF- κ B) pathways to block angiogenesis. Administration of gedunin suppressed the development of HBP carcinomas by inhibiting PI3K/Akt and NF- κ B pathways through the inactivation of Akt and inhibitory kappa B kinase (IKK), respectively. Immunoblot and molecular docking interactions revealed that inhibition of these signaling pathways may be mediated via inactivation of AR by gedunin. Gedunin blocked angiogenesis by down-regulating the expression of miR-21 and the pro-angiogenic factors vascular endothelial growth factor and hypoxia inducible factor-1 alpha (HIF-1 α). In conclusion, the results of the present study provide compelling evidence that gedunin prevents progression of hamster buccal pouch (HBP) carcinomas via inhibition of the kinases Akt, IKK, and AR, and the oncogenic transcription factors NF- κ B and HIF-1 α to block angiogenesis.

Keywords Gedunin · Angiogenesis · Aldose reductase · Phosphatidyl inositol-3-kinase · Akt · Nuclear factor kappa B

Introduction

Aberrant activation of oncogenic signaling pathways has been consistently associated with the acquisition of hallmarks of cancer including cell proliferation, apoptosis evasion, invasion, and angiogenesis [1, 2]. In particular, PI3K/Akt/mToR and NF- κ B signaling pathways are the most dysregulated in a wide range of malignant neoplasms [3, 4]. Phosphatidylinositol 3-kinase (PI3K) is an upstream lipid kinase activated by various growth factors such as insulin-like growth factor (IGF), epidermal growth factor (EGF), and vascular endothelial growth factor (VEGF) via receptor tyrosine kinases. Phosphorylation is an important event for PI3K activation and tightly regulated by the tumor suppressor gene PTEN [5, 6]. Activation of PI3K recruits protein kinase B/Akt to the plasma membrane. Akt is a serine/threonine kinase, phosphorylated by phosphatidylinositol-dependent kinase (PDK) 1 and 2 at threonine 308 and serine 473, respectively. Activated Akt in turn phosphorylates multiple downstream proteins including mammalian target of rapamycin (mToR) and inhibitory kappa B kinase (IKK) [7, 8].

NF- κ B, a transcription factor downstream of Akt, regulates diverse cellular activities including growth and development. NF- κ B exists as a heterodimer of NF- κ B p50 and NF- κ B p65 subunits sequestered in the cytoplasm by inhibitory kappa B (I κ B) in unstimulated cells. In stimulated cells, I κ B is phosphorylated by inhibitory kappa B kinase complex followed by ubiquitination and proteasomal degradation, releasing NF- κ B that translocates to the nucleus, and transactivates target genes responsible for tumor progression [9, 10].

✉ Siddavaram Nagini
s_nagini@yahoo.com; snlabau@gmail.com

¹ Department of Biochemistry and Biotechnology, Faculty of Science, Annamalai University, Annamalainagar 608 002, Tamil Nadu, India

² Biochemistry Division, National Institute of Nutrition, Hyderabad 500 007, India

³ Medicinal Chemistry Research Division, Vishnu Institute of Pharmaceutical Education and Research, Narsapur, India

Table 1 Body weight gain, food consumption, tumor incidence, and histopathological changes in control and experimental animals (mean±SD; n=6)

Group	Treatment	Body weight gained (g)	Food consumed g/hamster/day	Tumor incidence	Hyperplasia	Dysplasia	SCC (%)
1.	DMBA	45.6±4.9*	7.37±0.8	6/6 (100 %)	+++	+++	100
2.	DMBA+gedunin (1 µg/kg bw)	48.7±5.3	7.43±0.9	5/6 (83.3 %)	+++	+++	83.3
3.	DMBA+gedunin (10 µg/kg bw)	56.5±4.6**	7.61±0.6	3/6 (50 %)	+++	++	50
4.	DMBA+gedunin (100 µg/kg bw)	65.0±5.7**	7.88±0.7	0/6 (0 %)	+	–	–
5.	Control	68.7±6.5	7.96±0.8	–	–	–	–

+ mild, ++ moderate, +++ severe, – no change, SCC squamous cell carcinoma

*Significantly different from control ($p<0.05$)

**Significantly different from group 1 ($p<0.05$)

Reciprocal activation of PI3K/Akt/mTOR and NF- κ B signaling pathways is recognized to promote angiogenesis by activating hypoxia inducible factor-1 alpha (HIF-1 α), a master regulatory transcription factor and enhancer of vascular endothelial growth factor (VEGF) signaling [11]. Aldo-keto reductase (AR, AKR1B1; EC1.1.1.21), an enzyme that catalyzes the reduction of lipid aldehydes and stimulates redox sensitive oncogenic pathways including NF- κ B and PI3K/Akt, mediates hypoxic signals leading to angiogenesis [12, 13]. miR-21, an oncomiR, is known to activate the PI3K/Akt pathway by targeting PTEN and promote angiogenesis [14]. Therefore, identification of phytochemicals that target the AR-NF- κ B-PI3K/Akt axis has emerged as a promising strategy for blocking tumor angiogenesis.

Azadirachta indica, commonly known as neem with its rich array of limonoids, has attracted the focus of research attention for its wide spectrum of medicinal properties, predominantly anticancer effects [15, 16]. Extensive investigations from this laboratory have provided evidence for the anticancer properties of neem leaf extracts and the neem limonoids azadirachtin and nimbolide in cancer cell lines in vitro and in animal tumor models in vivo [17–21]. Of late, the neem limonoid gedunin (10-(furan-3-yl), penta methyl dioxo tetradecahydronaphto oxireno isochromen-6yl acetate) has been shown to exhibit antiproliferative properties against diverse cancer cell lines by modulating various oncogenic signaling pathways [22–25]. However, the cellular and molecular targets of gedunin have not been

Fig. 1 H&E stained regions of buccal pouch mucosa of control and experimental animals ($\times 40$). **a** and **b** Buccal pouch epithelium from DMBA and DMBA+gedunin (1 µg/kg bw) administered group exhibiting well-differentiated SCC with extensive infiltration into connective tissue, respectively. **c** Buccal pouch epithelium from DMBA+gedunin (10 µg/kg bw) administered group exhibiting moderate dysplasia. **d** Buccal pouch epithelium from DMBA+gedunin (100 µg/kg bw) administered group exhibiting mild hyperplasia. **e** Control animals exhibiting normal buccal pouch

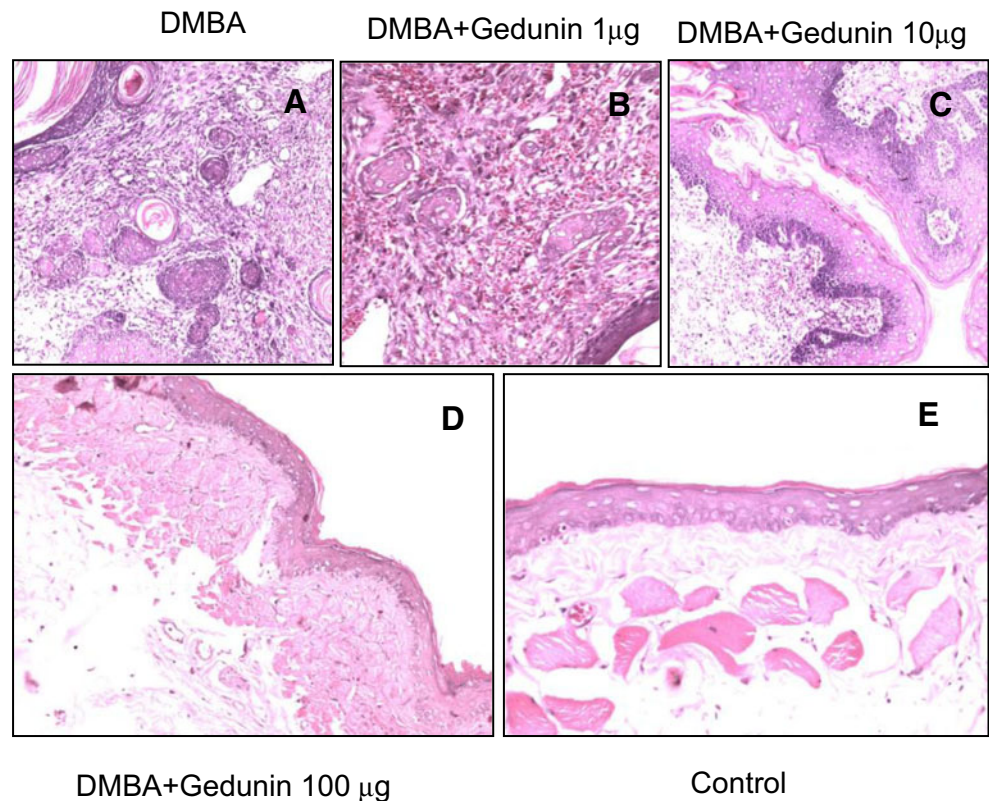
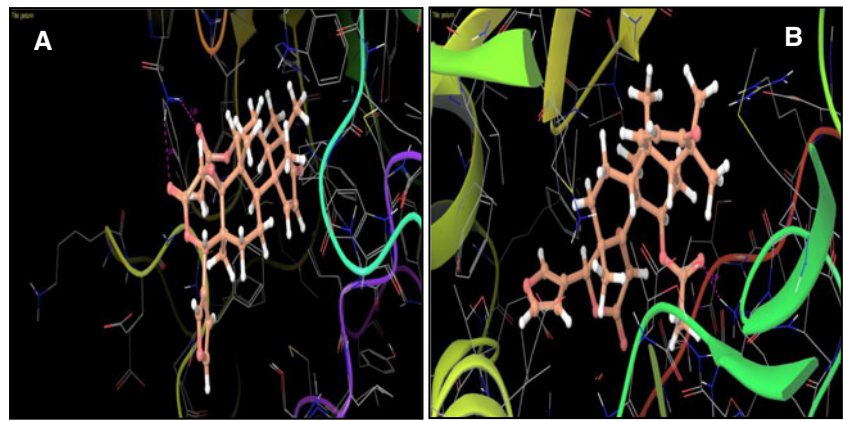


Fig. 2 Docking of gedunin with Aldose reductase and Akt2. **a** Gedunin forms hydrogen bond (Pink dotted line) with Gln 49 of AR. **b** Gedunin forms hydrogen bond (Pink dotted line) with Lys 277 of Akt2



identified in vivo. The present study was therefore undertaken to investigate the effects of gedunin on AR-PI3K/Akt/mTOR and NF- κ B signaling pathways as well as HIF-1 α -mediated VEGF signaling in the hamster buccal pouch (HBP) carcinogenesis model, a well characterized animal system for chemointervention studies.

Materials and methods

Chemicals

Acrylamide, bis-acrylamide, bovine serum albumin (BSA), bromophenol blue, diethylpyrocarbonate (DEPC),

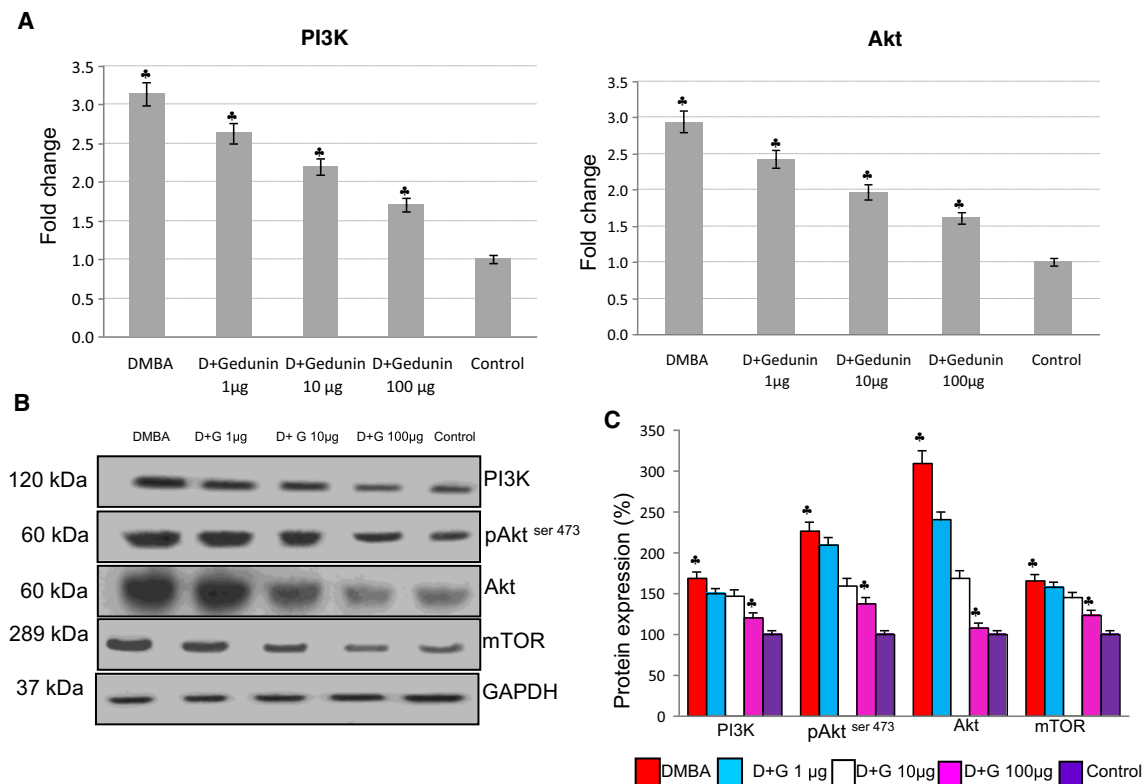
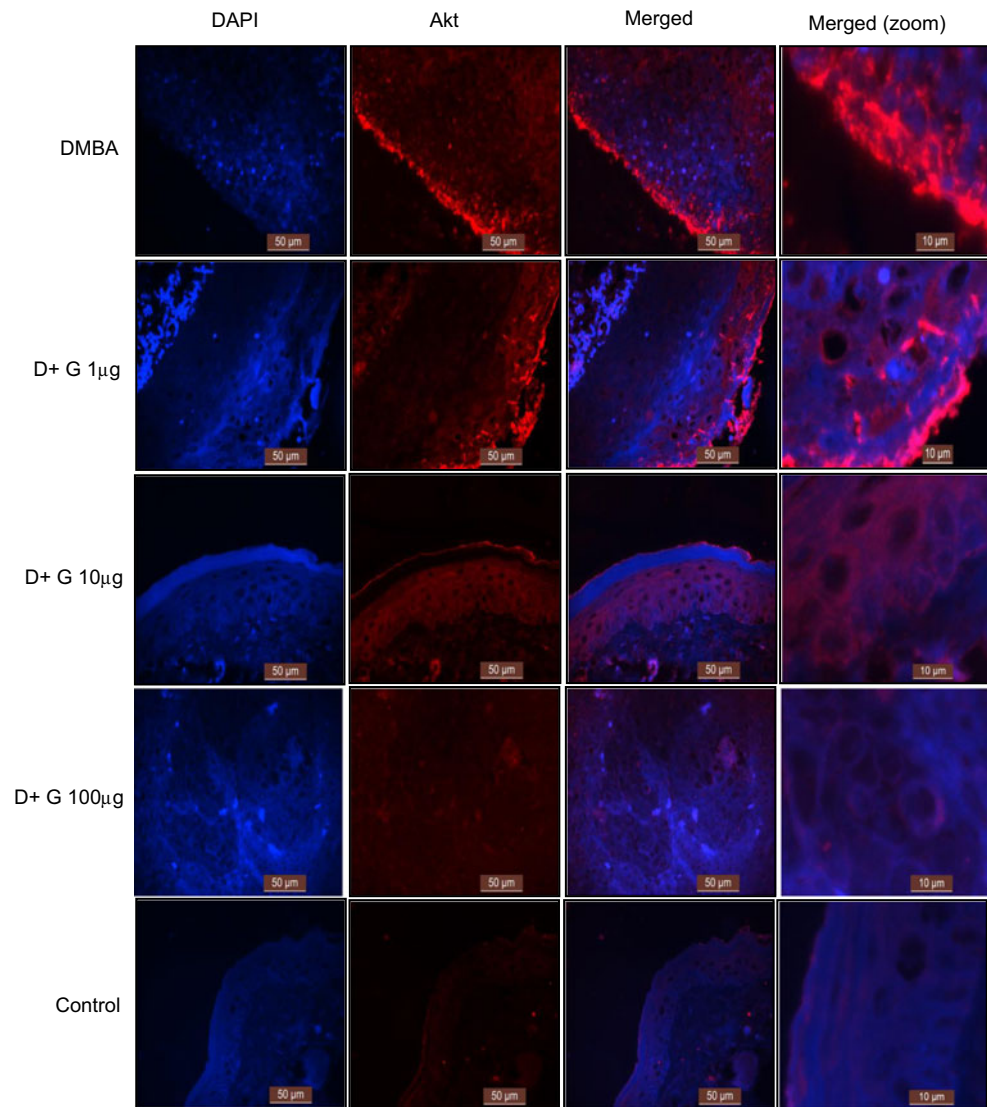


Fig. 3 Dose-response effect of gedunin on the expression of PI3K, Akt, and mTOR in control and experimental animals (mean \pm SD; $n=3$). **a** Quantitative RT-PCR analysis of PI3K and Akt. cDNA individually generated from the buccal pouch RNA of biological replicates was subjected to qRT-PCR analysis. Relative mRNA expression for each gene was determined and normalized to the average transcript expression of internal control GAPDH. The fold change in transcript expression for each gene was determined using the $2^{-\Delta\Delta C_t}$ method.

Data are the mean \pm SD of two separate experiments. Statistical significance was determined by Mann-Whitney test ($p<0.05$). **b** Immunoblot analysis of PI3k/Akt pathway. GAPDH was used as loading control. **c** Densitometric analysis. The protein expression from control lysates for three determinations was designated as 100 % in the graph. Significantly different from control ($p<0.01$) by Mann-Whitney test (\clubsuit). Significantly different from DMBA group ($p<0.05$) (asterisk)

Fig. 4 Immunofluorescence of Akt. Immunofluorescence of Akt in control and experimental animals (63×). Increased Akt expression observed in animals painted with DMBA and DMBA+gedunin 1 and 10 µg/kg.bw. Decreased Akt expression observed in animals treated with gedunin at 100 µg/kg bw. Lower Akt expression observed in control group compared to DMBA group



DMBA, dithiothreitol (DTT), ethylene glycol-bis (2-aminoethylether)-N,N,N',N'-tetraacetic acid (EGTA), 2-mercaptoethanol, [4-(2-hydroxyethyl)-1-piperazinyl]-ethane sulfonic acid (HEPES), phenylmethylsulfonyl fluoride (PMSF), sodium dodecyl sulfate (SDS), N,N,N',N'-tetramethylene diamine (TEMED), and TRIzol were obtained from Sigma Chemical Company, USA. SYBR Green PCR master mix was obtained from Applied Biosystems, USA. Gedunin was procured from Tocris Biosciences. Primers were purchased from Sigma Genosys, USA. p-Akt^{Ser473}, p-NFκB p65^{Ser536}, p-VEGFR2^{Tyr1175}, and mTOR antibodies were obtained from Cell Signaling Technology (MA, USA). Akt, cleaved caspase-3, cleaved caspase-9, HIF-1α, NFκB p50, NFκB p65, PI3K, p-IκB-α, IκB-α, IKKβ, VEGF, VEGFR2, and horseradish peroxidase-conjugated anti-rabbit, anti-goat, and anti-mouse secondary antibodies were obtained from Santa Cruz Biotechnology, USA.

Alexafluor-488 conjugated anti-rabbit and Alexafluor-555 conjugated anti-mouse antibodies were obtained from Molecular Probes, Inc. (Eugene, OR, USA). All other reagents used were of analytical grade.

Animals and ethics statement

Two-month-old male Syrian hamsters with average body weight of 100±12 g were obtained from the National Centre for Laboratory Animal Sciences, National Institute of Nutrition, India. The animals were housed three to a polypropylene cage and provided with standard pellet diet (Sai Enterprisei, Chennai, India) and water ad libitum. The animals were maintained in a temperature of 22±2 °C and 50 % humidity with an alternating 12-h light/dark cycle according to the guidelines of Indian Council of Medical Research. The study protocol was approved by the Institutional Animal Ethics Committee, Annamalai

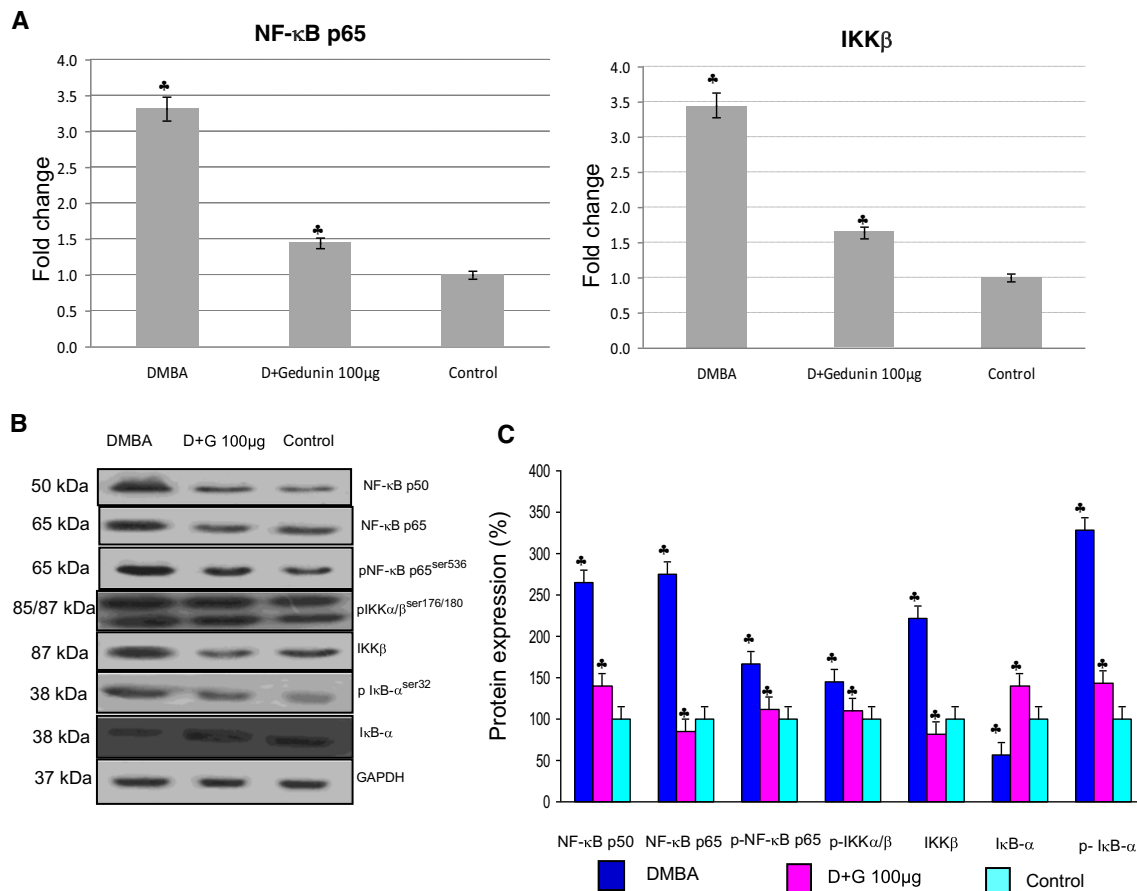


Fig. 5 Effect of gedunin on the mRNA and protein expression on NF-κB p50, NF-κB p65 and IKKα/β, and IκB in control and experimental animals (mean±SD; $n=3$). **a** Quantitative RT-PCR analysis of NF-κB p65 and IKKβ. cDNA individually generated from the buccal pouch RNA biological replicates was subjected to qRT-PCR analysis. Relative mRNA expression for each gene was determined and normalized to the average transcript expression of internal control GAPDH. The fold change in transcript expression for each gene was determined using the

$2^{-\Delta\Delta Ct}$ method. Data are the mean±SD of two separate experiments. Statistical significance was determined by Mann-Whitney test ($p<0.05$). **b** Immunoblot analysis of NF-κB pathway. GAPDH was used as loading control. **c** Densitometric analysis. The protein expression from control lysates for three determinations was designated as 100 % in the graph. Significantly different from control ($p<0.01$) by Mann-Whitney test (*). Significantly different from DMBA group ($p<0.05$) (asterisk).

University and conducted according to the guidelines laid down by the Committee for the Purpose of Control and Supervision on Experiments on Animals (CPCSEA).

Treatment schedule

The animals were randomized into experimental and control groups and divided into five groups of six animals each. In group 1, the right buccal pouches of hamsters were painted with 0.5 % DMBA in liquid paraffin three times a week for 14 weeks as previously described [22]. Groups 2–4 animals received in addition to DMBA, intragastric administration of gedunin at a concentration of 1, 10, and 100 μg/kg bw, respectively. Group 5 animals received basal diet alone and served as an untreated control. The experiment was terminated at 14 weeks, and all animals were sacrificed by cervical dislocation after an overnight fast. The buccal pouch tissues were immediately subdivided and processed for distribution to each experiment.

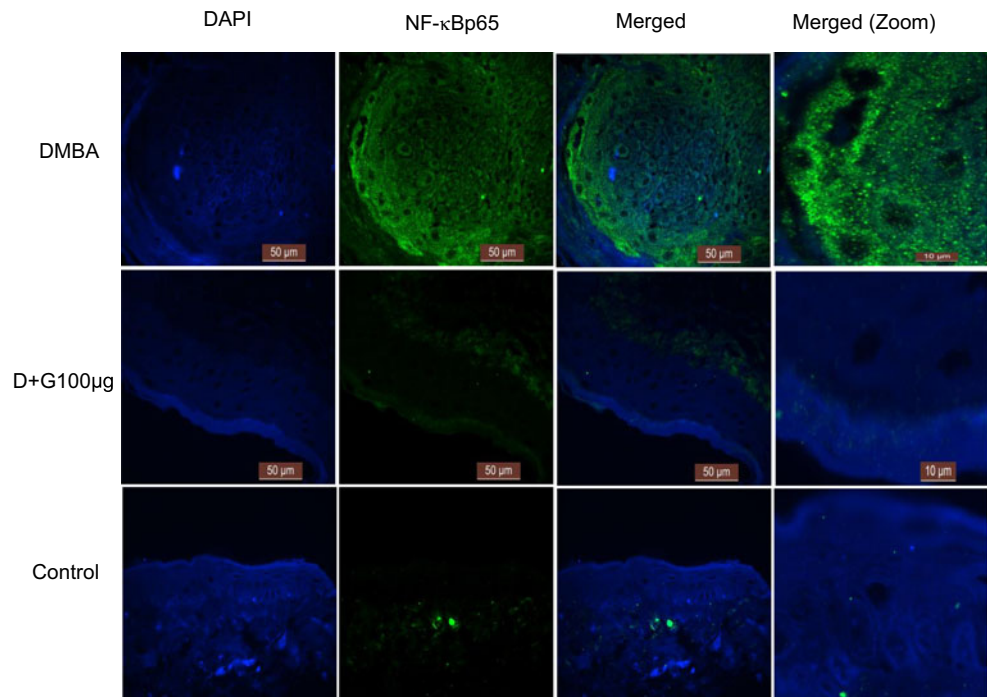
Histopathology

The buccal pouch tissues were fixed in 10 % formalin, embedded in paraffin blocks, and mounted on polylysine-coated glass slides. Tissue sections were stained with hematoxylin and eosin. Hyperplasia, dysplasia, and squamous cell carcinoma were diagnosed.

RNA extraction and quantitative real-time RT-PCR analysis

Total RNA was isolated from buccal pouch tissue samples using TRIzol reagent as described previously [23]. The amount of RNA was quantified by measuring absorbance at 260 and 280 nm on Biophotometer. Five micrograms of isolated total RNA was reverse-transcribed to complementary DNA (cDNA) in a reaction mixture containing 4 μl of 5× reaction buffer, 2 μl of dNTPs mixture (10 mM),

Fig. 6 Immunofluorescence of NF- κ B p65. Immunofluorescence of NF- κ B p65 in control and experimental animals (63 \times). Increased NF- κ B p65 expression observed in animals painted with DMBA. Decreased NF- κ B p65 expression observed in animals treated with gedunin at 100 μ g/kg.bw. Lower NF- κ B p65 expression observed in control group compared to DMBA group



20 U of RNase inhibitor, 200 U of avian-myeloblastosis virus (AMV) reverse transcriptase, and 0.5 μ g of oligo(dT) primer (Promega, WI, USA) in a total volume of 20 μ l. Gene expression levels were quantified using StepOne Plus thermocycler (Applied Biosystems). cDNA was amplified using power SYBR Green master mix (Invitrogen) as per the manufacturer's instructions. The following cDNA amplification program was used: 95 $^{\circ}$ C for 5 min, 40 cycles of 30 s at 95 $^{\circ}$ C, 30 s at 52 to 60 $^{\circ}$ C (based on the target), and 60 s at 72 $^{\circ}$ C. GAPDH was used as internal control. Comparative Ct method was used to calculate the relative quantitative fold change.

miRNA isolation

MicroRNA (miRNA) was isolated by miRNeasy minikit method as per the manufacturer's instructions and quantified at 260 and 280 nm using a Biophotometer. cDNA was synthesized by NcodeTM VILOTM miRNA cDNA synthesis kit method following manufacturer's instructions. miRNA expression levels were quantified using StepOne Plus thermocycler (Applied Biosystems).

Protein extraction and immunoblotting

The buccal pouch tissue (150 mg) was homogenized using lysis buffer containing 62.5 mM Tris (pH 6.8), 10 mM HEPES (pH 7.9), 10 mM KCl, 0.1 mM EDTA, 0.1 mM EGTA, 1 mM DTT, 0.5 mM PMSF, protease inhibitor cocktail, and 10 % SDS. The homogenate was

centrifuged at 14,000 \times g at 4 $^{\circ}$ C for 20 min. The protein concentrations were measured by the method of Bradford [24]. Protein extracts (50 μ g) were loaded onto SDS-PAGE, and the proteins after separation were transferred to nitrocellulose membrane. The blots were incubated for 1 h in a solution containing 1 \times PBS and 5 % nonfat dry milk to avoid nonspecific binding. The membranes were then probed with primary antibody diluted according to the manufacturer's instructions overnight at 4 $^{\circ}$ C. After washing, the blots were incubated with secondary antibody for 1 h followed by extensive washes with high and low salt buffers. The protein bands were visualized using enhanced chemiluminescence, followed by densitometry scanning on IISP flatbed scanner and quantitated with Total Lab 1.11 software.

Immunofluorescence

The tissue sections were deparaffinized by incubating in xylene for 10 min followed by dehydration in decreasing grades of alcohol. Deparaffinized sections were boiled in 0.01-M sodium citrate buffer pH 6.0 for 10 min and blocked with blocking solution (3 % BSA). The slides were then washed with PBS and incubated with primary antibodies overnight at 4 $^{\circ}$ C. Tissue sections were washed with PBS and incubated with Alexafluor-conjugated secondary antibody for 1 h. The sections were mounted in medium containing 4,6-diamidino-2-phenylindole (DAPI; #1500, Vector Laboratories, Burlingame, CA, USA) and visualized using a Leica laser microscope (LMD6000, Leica microsystems, Germany).

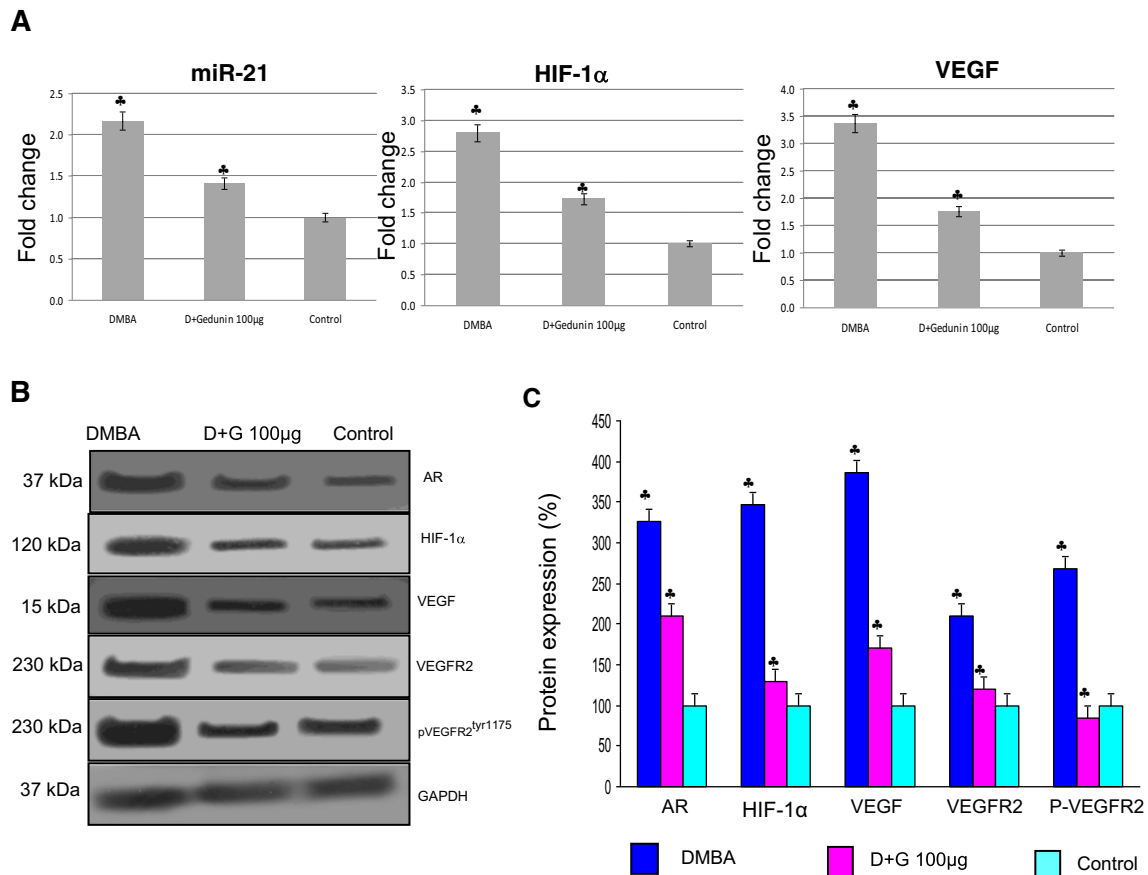


Fig. 7 Effect of gedunin on the mRNA and protein expression on AR, HIF-1 α , VEGF, VEGFR2, and miR21 in control and experimental animals (mean \pm SD; $n=3$). **a** Quantitative RT-PCR analysis of miR-21, HIF-1 α , and VEGF. cDNA individually generated from the buccal pouch RNA biological replicates was subjected to qRT-PCR analysis. Relative mRNA expression for each gene was determined and normalized to the average transcript expression of internal control GAPDH. The fold change in transcript expression for each gene was determined using the

$2^{-\Delta\Delta Ct}$ method. Data are the mean \pm SD of two separate experiments. Statistical significance was determined by Mann-Whitney test ($p<0.05$). **b** Immunoblot analysis of angiogenesis. GAPDH was used as loading control. **c** Densitometric analysis. The protein expression from control lysates for three determinations was designated as 100 % in the graph. Significantly different from control ($p<0.01$) by Mann-Whitney test (\clubsuit). Significantly different from DMBA group ($p<0.05$) (asterisk)

Microvascular density (MVD)

Microvascular density was analyzed by immunohistochemical staining with anti-CD34 antibody. The areas of highest neovascularization were located, and the images captured in a minimum of five different fields. Microvessels were counted by two independent investigators and the data represented as number of vessels/field of view.

Molecular docking

Molecular docking was done by Schrodinger suite 2013. 3D structure of gedunin (CID5701985) was retrieved from PubChem and minimized with OPLS-2005 force field (optimized potentials for liquid simulations), the stable energy conformation taken for docking studies. X-ray crystal structure of proteins Aldose reductase (1PWM) and Akt2 (2JDO) was downloaded from Protein Data Bank (PDB) and minimized by OPLS-2005 force field. Docking was done by Glide-XP module.

Post-docking calculations for the docked complexes were performed by using Prime MM/GBSA (molecular mechanics-based generalized born/surface area) module of Schrodinger suite.

Statistical analysis

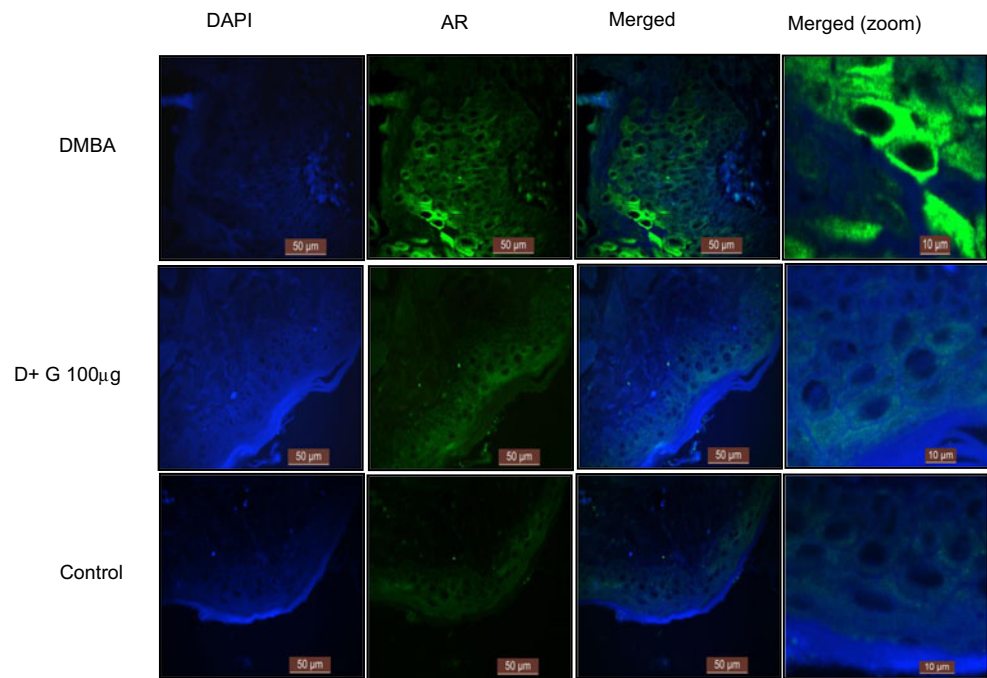
Statistical analysis was carried out using ANOVA and a non-parametric Mann-Whitney test (Statsdirect, UK). A probability value of less than 0.05 was considered significant.

Results

Body weight, food consumption, tumor incidence, and histopathological observations

Table 1 summarizes the body weight gain, food consumption, tumor incidence, and histopathological changes in control and experimental groups. The average body weight gain was

Fig. 8 Immunofluorescence of AR. Immunofluorescence of AR in control and experimental animals (63×). Increased AR expression observed in animals painted with DMBA. Decreased AR expression observed in animals treated with gedunin at 100 µg/kg bw. Lower AR expression observed in control group compared to DMBA group



significantly decreased in DMBA (group 1) animals compared to control (group 5). Intra-gastric administration of gedunin increased the final body weight in groups 2–4 animals compared to group 1. The average food intake per day was approximately 7.6 g. The amount of diet consumed by hamsters in groups 1–5 was not significantly different. In DMBA-treated animals, tumor incidence was 100 %. These tumors were large, exophytic, and histologically identified as well-differentiated squamous cell carcinomas (SCC) with prominent keratin pearls. In hamsters administered gedunin at concentrations of 1 µg/kg bw and 10 µg/kg bw, the incidence of SCC was reduced to 83.3 and 50 %, respectively. Histological examination of the buccal pouches exhibited varying degrees of preneoplastic and neoplastic lesions which are summarized in Table 1. Administration of gedunin at 100 µg/kg bw significantly ($p < 0.05$) reduced the tumor incidence, and only mild hyperplasia was observed in the buccal pouches of these animals. The epithelium of control hamsters was normal, intact, and continuous (Fig. 1).

Molecular docking study

We first investigated the docking interactions of gedunin with various upstream signaling kinases and oncogenic transcription factors. We found that gedunin stably binds with aldose reductase and Akt2 (Fig. 2). Gedunin binds on the active site of AR at Gln 49 residue, and its docking score and binding energies were -7.08 and 44.66 , respectively. Similarly, gedunin also binds with Akt 2 kinase domain at Lys 277 with docking score of -1.76 and binding energy of -39.05 . Based on these *in silico* studies, we next investigated whether

gedunin has any effects on the PI3K/Akt/mTOR pathway in the DMBA-induced HBP carcinomas.

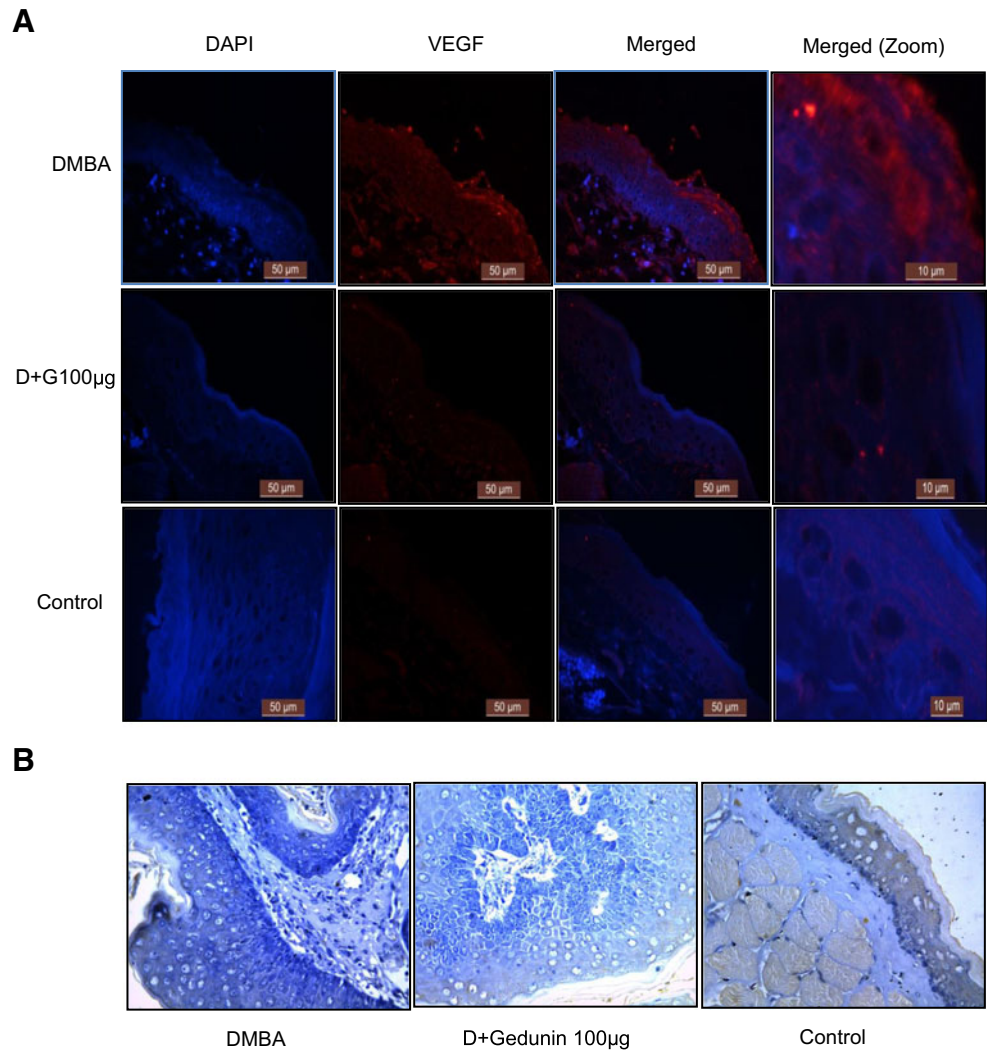
Gedunin abrogates PI3K/Akt/mTOR signaling

To confirm the leads from the docking studies, we first examined the expression of PI3K and Akt and their downstream target mTOR in control and experimental groups by quantitative RT-PCR and western blotting. Our results revealed that administration of gedunin significantly ($p < 0.05$) reduced the expression of PI3K, Akt, pAkt^{ser473}, and mTOR compared to DMBA-painted animals at all concentrations tested (1, 10, and 100 µg/kg bw), with 100 µg/kg bw gedunin exerting more significant effects (Fig. 3). Immunofluorescence analysis further confirmed that gedunin mediates its effects via Akt signaling (Fig. 4). Since the highest dose of gedunin showed significant tumor inhibitory effect, we used only this group for further analysis.

Gedunin inhibits NF-κB signaling

Since PI3K/Akt pathway acts as the chief upstream regulator of the transcription factor NF-κB and its activation through a p38/IKKα-dependent or an IKKβ-dependent mechanism, we next examined the effect of gedunin on the expression of key molecules involved in NF-κB signaling. Our results revealed that intra-gastric administration of gedunin significantly ($p < 0.05$) downregulated the expression of IKKβ, NF-κB p50, and NF-κB p65 in DMBA-painted hamsters compared to control (Fig. 5). Investigation of the mechanism underlying NF-κB down-regulation revealed that gedunin reduced the expression

Fig. 9 a Immunofluorescence of VEGF. Immunofluorescence of VEGF in control and experimental animals (63 \times). Increased VEGF expression observed in animals painted with DMBA. Decreased VEGF expression observed in animals treated with gedunin at 100 $\mu\text{g}/\text{kg}$ bw. Lower VEGF expression observed in control group compared to DMBA group. **b** Effect of gedunin on microvascular density. Microvascular density in control and experimental animals ($\times 40$)



of p-I κ B α^{ser32} by downregulating p-IKK α/β ser176/180 and preventing nuclear translocation of NF- κ B. Both immunoblot and immunofluorescence studies (Fig. 6) confirmed that gedunin blocks nuclear translocation of NF- κ Bp65. Gedunin also prevents the phosphorylation of NF- κ Bp65 at ser536 thereby inhibiting the transcriptional activity of NF- κ B.

Gedunin downregulates aldose reductase expression

Since aldose reductase is recognized to play a major role in the activation of NF- κ B pathway via PI3K/Akt signaling, we next examined whether gedunin has any effect on the expression of AR by western blotting and immunofluorescence. We found that administration of gedunin significantly ($p < 0.05$) decreased the expression of AR compared to DBMA group (Figs. 7 and 8). This was associated with decreased expression of miR-21. Results from docking studies as well as protein expression analysis confirmed that gedunin is a potent AR inhibitor.

Gedunin suppresses angiogenesis

Inhibitors of AR are known to block angiogenesis. We next sought to investigate whether gedunin-induced AR inhibition was associated with changes in the expression of key molecules regulating angiogenesis. The results revealed significant ($p < 0.05$) downregulation of HIF-1 α , VEGF, VEGFR2, and p-VEGFR2^{Tyr1175} following gedunin administration (Figs. 7 and 9). We further assessed the microvascular density (MVD), a characteristic feature of angiogenesis by immunohistochemistry (Fig. 9). While DMBA-painted hamsters showed high vasculature with a mean MVD of 210 compared to control animals, administration of gedunin significantly reduced the vasculature.

Discussion

Topical application of DMBA induced well-differentiated squamous cell carcinomas with high tumor burden.

Administration of gedunin significantly reduced tumor incidence and preneoplastic lesions in a dose-dependent manner. In particular, 100 $\mu\text{g}/\text{kg}$ bw of gedunin showed maximum efficacy as evidenced by inhibition of SCC development as well as dysplastic lesions that are indicative of preneoplasia. These results substantiate the antiproliferative effects of gedunin documented in a panel of cancer cell lines [25–28]. However, the effect of gedunin on angiogenesis, a hallmark of tumor progression, has not been investigated. In the present study, we report that gedunin modulates the oncogenic signaling pathways PI3K/Akt/mTOR and NF- κ B that drive angiogenesis in the DMBA-induced HBP carcinogenesis model.

PI3K/Akt/mTOR signaling is one of the most dysregulated pathways in diverse malignancies [29, 30]. In a previous study, we reported aberrant activation of the PI3K/Akt pathway in the HBP model [31]. Several phytochemicals and synthetic inhibitors have been documented to specifically target the PI3K/Akt/mTOR signaling pathway [5, 8, 32]. The findings of the current study demonstrate that gedunin inhibits PI3K/Akt/mTOR signaling by stably binding with the kinase domain of Akt2, an interaction that could prevent the activation of the downstream targets of Akt including mTOR and IKK. The IKK complex consists of two catalytic subunits, IKK α and IKK β and a regulatory subunit NEMO. IKK α and IKK β are essential for phosphorylating I κ B [33]. In the present study, gedunin abrogated NF- κ B signaling by inhibiting phosphorylation and degradation of IKK α/β , which in turn blocked nuclear translocation of NF- κ B. Gedunin also restrained the transcriptional activity of NF- κ B by preventing its phosphorylation at ser⁵³⁶.

Abrogation of the PI3K/Akt and NF- κ B pathways by gedunin was associated with inhibition of AR and downregulation of miR-21 expression. Molecular docking studies revealed that gedunin inhibits AR by stably binding to Gln49 on the active site. There is substantial evidence to indicate that inhibition of AR inactivates PI3K/Akt and NF- κ B signaling [12, 13]. In colon cancer cells, AR inhibition prevented EGF-induced phosphorylation of PI3K, Akt, and mTOR and downregulated miR-21 [34, 35]. Several phytochemicals that inhibit PI3K/NF- κ B signaling including curcumin and resveratrol have also been shown to inhibit AR and miR-21 expression [36–39]. Recently, Shin et al. [40] reported a correlation between siRNA-induced abrogation of NF- κ B and downregulation of miR-21 expression in gastric cancer. Inhibition or ablation with AR specific siRNA prevented hypoxia-induced proliferation and HIF-1 α -mediated angiogenesis [41, 42].

Extensive investigations have revealed that AR inhibitors are novel anti-angiogenesis agents. The results of the present study demonstrate that gedunin inhibits angiogenesis as evidenced by decreased microvasculature in the hamster buccal pouch and by suppressing the expression of HIF-1 α , VEGF, VEGFR2, and p-VEGFR2^{Tyr1175}. This inhibitory effect may

be due to blockade of PI3K/Akt/mTOR and NF- κ B signaling by gedunin.

Conclusion

In conclusion, the results of the present study provide compelling evidence that gedunin prevents progression of HBP carcinomas via inhibition of kinases such as Akt, IKK, and AR, and the oncogenic transcription factors NF- κ B and HIF-1 α to block angiogenesis.

Acknowledgments Financial support from the Indian Council of Medical Research, New Delhi, India, in the form of a Senior Research Fellowship to Mr. Kranthi Kiran Kishore T. is gratefully acknowledged.

Conflicts of interest None

Authors' contributions SN, GBR, and TKK designed the experiments. TKK, GR, and GDR performed the experiments and analyzed the data. SN, TKK, and GBR were involved in the preparation of the manuscript.

References

1. Yedida GR, Nagini S, Mishra R. The importance of oncogenic transcription factors for oral cancer pathogenesis and treatment. *Oral Surg Oral Med Oral Pathol Oral Radiol.* 2013;116:179–88.
2. Sever R, Brugge JS. Signal transduction in cancer. *Cold Spring Harb Perspect Med.* 2015;5:4.
3. Davis WJ, Lehmann PZ, Li W. Nuclear PI3K signaling in cell growth and tumorigenesis. *Front Cell Dev Biol.* 2015;3:24.
4. Chaturvedi MM, Sung B, Yadav VR, Kannappan R, Aggarwal BB. NF- κ B addiction and its role in cancer: 'one size does not fit all'. *Oncogene.* 2011;30:1615–30.
5. Porta C, Paglino C, Mosca A. Targeting PI3K/Akt/mTOR signaling in cancer. *Front Oncol.* 2014;4:64.
6. Simpson DR, Mell LK, Cohen EE. Targeting the PI3K/AKT/mTOR pathway in squamous cell carcinoma of the head and neck. *Oral Oncol.* 2015;51:291–8.
7. Li W, Wang H, Kuang CY, Zhu JK, Yu Y, Qin ZX, et al. An essential role for the Id1/PI3K/Akt/NF κ B/survivin signalling pathway in promoting the proliferation endothelial progenitor cells in vitro. *Mol Cell Biochem.* 2012;363:135–45.
8. Sun ZJ, Chen G, Hu X, Zhang W, Liu Y, Zhu LX, et al. Activation of PI3K/Akt/IKK-alpha/NF-kappaB signalling pathway is required for the apoptosis-evasion in human salivary adenoid cystic carcinoma: its inhibition by quercetin. *Apoptosis.* 2010;15:850–63.
9. Bai D, Ueno L, Vogt PK. Akt-mediated regulation of NFkappaB and the essentialness of NFkappaB for the oncogenicity of PI3K and Akt. *Int J Cancer.* 2009;125:2863–70.
10. Shen HM, Tergaonkar V. NFkappaB signaling in carcinogenesis and as a potential molecular target for cancer therapy. *Apoptosis.* 2009;14:348–63.
11. Hussain AR, Ahmed SO, Ahmed M, Khan OS, Al Abdulmohsen S, Platanius LC, et al. Cross-talk between NF- κ B and the PI3-kinase/AKT pathway can be targeted in primary effusion lymphoma (PEL) cell lines for efficient apoptosis. *PLoS One.* 2012;7:e39945.

12. Tammali R, Reddy AB, Srivastava SK, Ramana KV. Inhibition of aldose reductase prevents angiogenesis in vitro and in vivo. *Angiogenesis*. 2011;14:209–21.
13. Tammali R, Saxena A, Srivastava SK, Ramana KV. Aldose reductase inhibition prevents hypoxia-induced increase in hypoxia-inducible factor-1 α (HIF-1 α) and vascular endothelial growth factor (VEGF) by regulating 26 S proteasome-mediated protein degradation in human colon cancer cells. *J Biol Chem*. 2011;286:24089–100.
14. Sicard F, Gayral M, Lulka H, Buscail L, Cordelier P. Targeting miR-21 for the therapy of pancreatic cancer. *Mol Ther*. 2013;21:986–94.
15. Biswas K, Chattopadhyay I, Banerjee RK. Biological activities and medicinal properties of neem (*Azadirachta indica*). *Curr Sci*. 2002;82:1336–45.
16. Subapriya R, Nagini S. Medicinal properties of neem leaves: a review. *Curr Med Chem Anticancer Agents*. 2005;5:149–56.
17. Harish Kumar G, Chandra Mohan KV, Jagannadha Rao A, Nagini S. Nimbolide, a limonoid from *Azadirachta indica* inhibits proliferation and induces apoptosis of human choriocarcinoma (BeWo) cells. *Invest New Drugs*. 2009;27:246–52.
18. Kavitha K, Vidya Priyadarsini R, Anitha P, Ramalingam K, Sakthivel R, Purushothaman G, et al. Nimbolide, a neem limonoid abrogates canonical NF- κ B and Wnt signaling to induce caspase-dependent apoptosis in human hepatocarcinoma (HepG2) cells. *Eur J Pharmacol*. 2012;681:6–14.
19. Vidya Priyadarsini R, Manikandan P, Harish Kumar G, Nagini S. The neem limonoids azadirachtin and nimbolide inhibit hamster cheek pouch carcinogenesis by modulating xenobiotic-metabolizing enzymes, DNA damage, antioxidants, invasion, and angiogenesis. *Free Radic Res*. 2009;43:492–504.
20. Harish Kumar G, Vidya Priyadarsini R, Vinothini G, Vidhya Letchoumy P, Nagini S. The neem limonoids azadirachtin and nimbolide inhibit cell proliferation and induce apoptosis in an animal model of oral oncogenesis. *Invest New Drugs*. 2010;28:392–401.
21. Priyadarsini RV, Murugan RS, Sripriya P, Karunakaran D, Nagini S. The neem limonoids azadirachtin and nimbolide induce cell cycle arrest and mitochondria-mediated apoptosis in human cervical cancer (HeLa) cells. *Free Radic Res*. 2010;44:624–34.
22. Kavitha K, Kranthi Kiran Kishore T, Bhatnagar RS, Nagini S. Cytomodulin-1, a synthetic peptide abrogates oncogenic signaling pathways to impede invasion and angiogenesis in the hamster cheek pouch carcinogenesis model. *Biochimie*. 2014;102:56–67.
23. Chomczynski P, Sacchi N. Single-step method of RNA isolation by acid guanidinium thiocyanate-phenol-chloroform extraction. *Anal Biochem*. 1987;162:156–9.
24. Bradford MM. A rapid and sensitive method for the quantitation of microgram quantities of protein utilizing the principle of protein-dye binding. *Anal Biochem*. 1976;72:248–54.
25. Hieronymus H, Lamb J, Ross KN, Peng XP, Clement C, Rodina A, et al. Gene expression signature-based chemical genomic prediction identifies a novel class of HSP90 pathway modulators. *Cancer Cell*. 2006;10:321–30.
26. Uddin SJ, Nahar L, Shilpi JA, Shoeb M, Borkowski T, Gibbons S, et al. Gedunin, a limonoid from *Xylocarpus granatum*, inhibits the growth of CaCo-2 colon cancer cell line in vitro. *Phytother Res*. 2007;21:757–61.
27. Kamath SG, Chen N, Xiong Y, Wenham R, Apte S, Humphrey M, et al. Gedunin, a novel natural substance, inhibits ovarian cancer cell proliferation. *Int J Gynecol Cancer*. 2009;19:1564–9.
28. Patwardhan CA, Fauq A, Peterson LB, Miller GC, Blagg BS, Chadli A. Gedunin inactivates the cochaperone p23 protein causing cancer cell death by apoptosis. *J Biol Chem*. 2013;288:7313–25.
29. Mabuchi S, Kuroda H, Takahashi R, Sasano T. The PI3K/AKT/mTOR pathway as a therapeutic target in ovarian cancer. *Gynecol Oncol*. 2015;137:173–9.
30. Pal I, Mandal M. PI3K and Akt as molecular targets for cancer therapy: current clinical outcomes. *Acta Pharmacol Sin*. 2012;33:1441–58.
31. Kowshik J, Giri H, Kishore TK, Kesavan R, Vankudavath RN, Reddy GB, et al. Ellagic acid inhibits VEGF/VEGFR2, PI3K/Akt and MAPK signaling cascades in the hamster cheek pouch carcinogenesis model. *Anticancer Agents Med Chem*. 2014;14:1249–60.
32. Strickland LR, Pal HC, Elmets CA, Afaq F. Targeting drivers of melanoma with synthetic small molecules and phytochemicals. *Cancer Lett*. 2015;359:20–35.
33. Hinz M, Scheidereit C. The I κ B kinase complex in NF- κ B regulation and beyond. *EMBO Rep*. 2014;15:46–61.
34. Saxena A, Tammali R, Ramana KV, Srivastava SK. Aldose reductase inhibition prevents colon cancer growth by restoring phosphatase and tensin homolog through modulation of miR-21 and FOXO3a. *Antioxid Redox Signal*. 2013;18:11249–62.
35. Saxena A, Shoeb M, Ramana KV, Srivastava SK. Aldose reductase inhibition suppresses colon cancer cell viability by modulating microRNA-21 mediated programmed cell death 4 (PDCD4) expression. *Eur J Cancer*. 2013;49:3311–9.
36. Zhang W, Bai W, Zhang W. MiR-21 suppresses the anticancer activities of curcumin by targeting PTEN gene in human non-small cell lung cancer A549 cells. *Clin Transl Oncol*. 2014;16:708–13.
37. Muthenna P, Suryanarayana P, Gunda SK, Petrash JM, Reddy GB. Inhibition of aldose reductase by dietary antioxidant curcumin: mechanism of inhibition, specificity and significance. *FEBS Lett*. 2009;583:3637–42.
38. Wang G, Dai F, Yu K, Jia Z, Zhang A, Huang Q, et al. Resveratrol inhibits glioma cell growth via targeting oncogenic microRNAs and multiple signaling pathway. *Int J Oncol*. 2015;46:1739–47.
39. Zhou C, Ding J, Wu Y. Resveratrol induces apoptosis of bladder cancer cells via miR-21 regulation of the Akt/Bcl-2 signaling pathway. *Mol Med Rep*. 2014;9:1467–73.
40. Shin VY, Jin H, Ng EK, Cheng AS, Chong WW, Wong CY, et al. NF- κ B targets miR-16 and miR-21 in gastric cancer: involvement of prostaglandin E receptors. *Carcinogenesis*. 2011;32:240–5.
41. Yadav UC, Srivastava SK, Ramana KV. Prevention of VEGF-induced growth and tube formation in human retinal endothelial cells by aldose reductase inhibition. *J Diabetes Complications*. 2012;26:369–77.
42. Liu LZ, Li C, Chen Q, Jing Y, Carpenter R, Jiang Y, et al. MiR-21 induced angiogenesis through AKT and ERK activation and HIF-1 α expression. *PLoS One*. 2011;6:e19139.